Study of the lower hybrid resonance frequency over the regions of gathering earthquakes using DEMETER data

D.I. Vavilov, D.R. Shklyar, E.E. Titova, Michel Parrot

Journal of Atmospheric and Solar-Terrestrial Physics 100-101 (2013) 1–12

Contents lists available at SciVerse ScienceDirect

Journal of Atmospheric and Solar-Terrestrial Physics

journal homepage: www.elsevier.com/locate/jastp

Study of the lower hybrid resonance frequency over the regions of gathering earthquakes using DEMETER data

D.I. Vavilov [a,b,*], D.R. Shklyar [b,c], E.E. Titova [b,d], M. Parrot [a]

[a] LPC2E/CNRS, 3A Avenue de la Recherche Scientifique, 45071 Orléans cedex 2, France
[b] Space Research Institute of RAS, Moscow, Russia
[c] Moscow Institute of Physics and Technology, Dolgoprudny, Russia
[d] Polar Geophysical Institute, Apatity, Murmansk region, Russia

ARTICLE INFO

Article history:
Received 24 March 2012
Received in revised form
18 March 2013
Accepted 20 March 2013
Available online 29 March 2013

Keywords:
Lower hybrid resonance frequency
VLF transmitter signals
LHR reflection
Earthquakes

ABSTRACT

Variations of plasma distribution and/or wave spectral features in the ionosphere were suggested by many authors as possible earthquake precursors, and the change of plasma density and temperature above seismic regions were reported in the literature. These quantities are known to influence the lower hybrid resonance (LHR) frequency profiles in the upper ionosphere and the magnetosphere, which, in turn, strongly affects the propagation of quasi-resonance VLF waves with frequencies f close to the maximum of the LHR frequency on the propagation path. This makes the VLF signals a tool of registration of ionospheric perturbations. Using the measurements from the DEMETER satellite for 3 yr we have calculated the maps of LHR frequency over the globe, and the maps of VLF spectral intensity at the frequencies of Alpha navigation transmitters. These maps demonstrate a significant dependence of the spectral intensity in the transmitter conjugate region on the relation between the signal frequency and the LHR frequency above the observation point. Then, using the DEMETER data and the earthquake database from the US geological survey server we have performed statistical analysis of the LHR frequency over seismic regions and found an appreciably different behaviour of the LHR frequency before earthquakes, as compared to its regular behaviour, for several seismic regions. Although this difference is statistically significant, in each particular case the ionospheric perturbations may be related to different processes in the Earth's atmosphere, ionosphere, and the magnetosphere, other than gathering earthquakes. Thus, the unexpected variations in the LHR frequency profile, revealed from the variations of VLF transmitter signals, should only be considered as one indicator in a list of possible earthquake precursors.

1. Introduction

Ionospheric perturbations prior to earthquakes have been in the focus of seismo-electromagnetic studies since their beginning in the 1970s (Larkina et al., 1984, 1989; Parrot and Lefeuvre, 1985; Serebryakova et al., 1992; Chmyrev et al., 1997). Many results on this subject obtained by the end of the last century were summarised in a comprehensive collection “Seismo Electromagnetics: Lithosphere–Atmosphere–Ionosphere Coupling” edited by Hayakawa and Molchanov (2002). The analysis of the VLF signals radiated by ground transmitters and received onboard the French DEMETER satellite revealed signal dropoffs connected with the occurrence of large earthquakes (the so-called scattering spot, Molchanov et al., 2006). Earthquake related drops in VLF signal phase and amplitude registered by ground-based receivers, and in signal amplitude measured onboard the DEMETER satellite have been indicated by Rozhnoi et al. (2007). VLF transmitter signal decreasing during a month before the earthquake near Sumatra has been reported by Solovieva et al. (2009).

It has soon been recognised that indirect effects of earthquake preparation processes on plasma distribution and wave spectrum registered above seismic region may be more pronounced than direct ones (Bošková et al., 1993). In particular, it has been shown that earthquake related plasma density perturbations in the ionosphere are essential for producing observable spectral peculiarities (Chmyrev et al., 2008). Physical mechanisms responsible for earthquake related wave and particle disturbances above seismic regions constitute the most important problem related to our study, which, however, is out of the scope of the present work. Yet, we should mention that gravity waves can be the “end” cause of ionospheric variations which transfer various kinds of disturbances from their origin into the ionosphere (and references therein Francis, 1975; Grigor'ev, 1999; Lee et al., 2008).

* Corresponding author at: Space Research Institute of RAS, Moscow, Russia
E-mail addresses: vavilov86@yandex.ru (D.I. Vavilov), david@iki.rssi.ru (D.R. Shklyar), lena.titova@gmail.com (E.E. Titova), mparrot@cnrs-orleans.fr (M. Parrot).

1364-6826/$ - see front matter © 2013 Elsevier Ltd. All rights reserved.
http://dx.doi.org/10.1016/j.jastp.2013.03.019

In this study, we suggest and substantiate a new indication of anomalous variations in the ionosphere. This indication consists in unusual change of VLF transmitter signal amplitude observed in the hemisphere opposite to that of the transmitter location, and serves as a warning of anomalous processes in the ionosphere above the observation region, of which a gathering earthquake can be one of the possible causes. In the next section we shortly describe some features of VLF transmitter signal propagation in the magnetosphere, which are essential for the monitoring that we suggest. In Section 3, we discuss the dependence of LHR frequency on the parameters of ionospheric plasma. Section 4 describes data acquisition and data analysis. Section 5 presents the maps of the LHR frequency and the maps of VLF spectral intensity at the frequencies of Alpha navigation transmitters obtained from DEMETER data. The LHR frequency above seismic regions, together with the method of estimation of its variations, are discussed in Section 6 based on the performed statistical analysis. Section 7 contains the discussion and the conclusions from the present study.

2. Some propagation properties of VLF transmitter signals

Propagation of fixed frequency VLF signals in near-Earth space possesses features similar to those of lightning-induced whistlers (Helliwell, 1965). A signal from a ground-based VLF transmitter initially propagates in the Earth-ionosphere waveguide partly leaking into the ionosphere. Due to a sharp increase of the wave refractive index at the upper boundary of the waveguide, the wave normal is almost vertical at the ionospheric level where the wave mode changes distinctly from free space mode to whistler mode in collisional plasma. Starting from the heights ~500–1000 km, the wave propagation is well described in the frame of geometrical optics.

Depending on the presence or absence of a duct, the wave propagation is quite different. The features of non-ducted propagation, which we consider as a more common case (see for example, Walter and Angerami, 1969; Cerisier, 1973; Collier et al., 2011), consist in a tendency of the wave normal to bend towards 90° with respect to the geomagnetic field, and transition to quasi-resonance regime of propagation which is characterised by an essential increase of the wave refractive index (Walker, 1976; Alekhin and Shklyar, 1980). As it is well known (Kimura, 1966), such waves cannot propagate in the region where the wave frequency f is below the lower hybrid resonance (LHR) frequency f_{LHR}. Thus, if a signal from ground-based VLF transmitter situated, say, in the Northern hemisphere propagates in non-ducted mode, and if the maximum of LHR frequency profile in the Southern hemisphere is above the wave frequency, then the wave will be magnetospherically reflected from the region where $f=f_R$

$$f_R^2=f_{\mathrm{LHR}}^2\frac{N^2}{N^2+f_p^2/f^2} \tag{1}$$

(see Shklyar et al., 2004 for details). Here N is the wave refractive index, f_p is the electron plasma frequency, and large refractive index assumes $N^2\gg f_p^2/f^2$. On the contrary, if the frequency of transmitter signal f is above the maximum of LHR frequency profile, then the signal will not be reflected and will reach the lower ionosphere. We thus see that the relation between transmitter signal frequency f and $(f_{\mathrm{LHR}})_{\max}$ above the satellite is crucial in determining whether or not the signal will be observed on a satellite like DEMETER orbiting between the upper-ionospheric and lower-ionospheric maxima of LHR frequency (Shklyar et al., 2010). Further on, we speak about the upper-ionospheric maximum of the LHR frequency which is essential in our consideration. Even if $f\lesssim(f_{\mathrm{LHR}})_{\max}$ so that wave effects prevent the total reflection, the signal amplitude below the LHR maximum will be smaller than in the case $f\gtrsim(f_{\mathrm{LHR}})_{\max}$. This feature constitutes a key point in the monitoring idea that we suggest. We should stress that even quasi-resonance low-frequency ($f\ll f_c$, where f_c is the electron cyclotron frequency) whistler-mode waves propagate (in the group sense) almost along the ambient magnetic field (Storey, 1953). Thus, the main property of non-ducted waves that we use is the LHR reflection, but not the deviation of trajectory from the magnetic field line.

3. Modification of LHR frequency profile in response to variations of ionospheric parameters

Earthquake related variations of ionospheric plasma density and temperature have been reported by many authors (see e.g. Gokhberg et al., 1983; Afonin et al., 1999; Hayakawa et al., 2000; Pulinets et al., 2003, 2004, and references therein). Of particular interest for the present work are the observations by Bošková et al. (1993) showing: (1) an increase in the light ion concentration over a narrow latitudinal region above the focus of the forthcoming earthquake and (2) a general increase in the light ion density in the relevant latitudinal region as a whole, at longitudes close to the future epicenter, as compared to other longitudes. Thereafter, Shklyar and Truhlik (1998), in terms of a simple qualitative model, have demonstrated that light ion profiles in the ionosphere are over-responsive to small variations of plasma parameters. Let us analyse how the variations of light ion distribution affect the LHR frequency profile in the upper ionosphere in more detail. To this end, we write the well known expression for the LHR frequency

$$f_{\mathrm{LHR}}^2=\frac{1}{M_{\mathrm{eff}}}\frac{f_c^2f_p^2}{f_p^2+f_c^2}, \tag{2}$$

where M_{eff} is the dimensionless effective ion mass determined by the relation

$$\frac{1}{M_{\mathrm{eff}}}=\frac{m_e}{n_e}\sum_{\mathrm{ions}}\frac{n_\alpha}{m_\alpha}. \tag{3}$$

Here n_e, m_e are the electron density and mass, respectively, n_α, m_α are the same for ions of species α, and summation is assumed over all ion species. The characteristic scale of electron cyclotron frequency variations in the upper ionosphere is of the order of thousand kilometers. Formula (2) then shows that the LHR frequency profile at the heights of low-orbiting (~500–1500 km) satellites is mainly determined by the behaviour of electron density $n_e\propto f_p^2$ and effective ion mass M_{eff}. It is worth mentioning that under condition $f_p^2\gg f_c^2$, which is often fulfilled in the upper ionosphere, the LHR frequency is determined only by M_{eff} and f_c.

Above the maximum of electron density, which is reached in the F region of the ionosphere, the electron and ion density profiles can be qualitatively approximated by the model of diffusive equilibrium (e.g. Angerami and Thomas, 1964). In this model, electron and ion height distributions are mainly determined by ion composition at the "base level" (~500 km) and electron and ion temperature profiles. As it has been underlined by Shklyar and Truhlik (1998), in the model of diffusive equilibrium, the light ion distribution is very sensitive to small variations of plasma parameters. The same must be true for the LHR frequency profile, since the light ion distribution affects most strongly the distribution of effective ion mass M_{eff} (see (3)), which in turn determines f_{LHR} according to (2). Thus, small variations of plasma parameters in the lower ionosphere can lead to significant changes in both the height and the magnitude of LHR maximum in the upper ionosphere.

4. Wave and particle experiments on DEMETER, and description of data analysis

The present study is based on the DEMETER satellite measurements. DEMETER was a French satellite designed to study ionospheric perturbations related to seismic and man-made activity. It was launched in June 2004 and operated until the end of 2010, orbiting on circular polar orbits, initially at the height of 710 km and then, beginning from December 2005, at the height of 660 km. Its payload consisted of wave and particle analysers. The satellite measured electromagnetic waves all around the Earth except in the auroral zones (Parrot et al., 2006). The frequency range for the electric field was from DC up to 20 kHz, most of which falls into the VLF band. Due to sun-synchronous type of DEMETER orbit, all measurements correspond to two local times: $LT \simeq 10:30$ and $LT \simeq 22:30$. There were two scientific modes of operation: a survey mode where frequency-time spectra of one electric and one magnetic component were computed onboard up to 20 kHz, and a burst mode when, in addition to the onboard computed spectra, waveforms of one electric and one magnetic field component were recorded, permitting spectrum evaluation up to 20 kHz. The burst mode allowed a spectral analysis with higher time and frequency resolution. During this mode of operation, the six components of the electromagnetic field were also recorded in the ELF range up to 1.25 kHz, which permitted the determination of all wave characteristics, and performing a wave propagation analysis (Santolík et al., 2006). Details of wave and plasma experiments onboard DEMETER can be found in Parrot et al. (2006) and Berthelier et al. (2006a, 2006b).

The Demeter Langmuir probe experiment (ISL) has been designed for in situ measurements of the bulk parameters of the ionospheric thermal plasma. It was composed of two electrodes: a cylindrical and a spherical electrode whose surfaces were divided in segments electrically isolated from each other. This segmentation was made for deriving the bulk velocity of plasma, in addition to the routinely measured electron density and temperature. The principle of the measurement technique is to vary the bias voltage applied to the Langmuir probe and to measure the current collected as a function of the applied voltage (i.e. to acquire the current–voltage (I–V) characteristic of the probe). The analysis of the (I–V) characteristic provides the following plasma parameters with their expected values along the orbit: electron density in the range $(10^8–5\times10^{11})$ m^{-3}, electron temperature (600–10 000 K), ion density (the same range as for electron density), and spacecraft potential (± 3 V). A complete voltage sweep is performed in 1 s, thus allowing to obtain the (I–V) characteristic every second providing 1 s time resolution of plasma bulk parameters. The time resolution of 1 s corresponds to about 7 km spatial resolution on the 700 km altitude DEMETER orbit (see Lebreton et al., 2006 for details).

The IAP instrument onboard DEMETER provided a nearly continuous survey of the main parameters of the thermal ion population. The operation principle is based on the combination of two different instruments. The first one is a retarding potential analyser and performs the energy analysis of the rammed ions from which one can retrieve the density and temperature of the major ions O^+, He^+ and H^+, as well as the component of their velocity along the line of sight of the analyser. The second one is an ion drift analyser that allows to determine the velocity direction of the rammed ions. Using the velocity value along the sight of the analyser, together with the arrival direction of the rammed ions, one can obtain the ion velocity vector in the satellite frame of reference and, finally, by subtracting the orbital ram velocity vector, the ion drift velocity vector in the Earth's frame of reference. Depending on the mode of operation, time resolution of the ion parameters is 2.317 s in Burst modes, 4.506 s in Survey 1 mode, and 4.429 s in Survey 2 mode (IAP Survey 1 mode corresponds to a medium energy resolution, and IAP Survey 2 corresponds to a high energy resolution). The ion densities are measured onboard in the range $(10^2–10^5)$ ions/cm^3 (see Berthelier et al., 2006b for details.)

For calculating the lower hybrid resonance frequency, two data sets were used: electron density measured by the Langmuir probe (ISL experiment), and ion densities measured by the Ion Plasma Analyser (IAP experiment). We should mention that for "ideal" measurements, the total ion density would be equal (in experiment, close) to electron density, which is the case for daytime measurements. However, for night-time measurements, these densities may disagree. Then, there are two ways for calculating the LHR frequency. The first is to take the absolute ion densities as the basic quantities, and to put electron density equal to the sum of ion densities. The second possibility is to use electron density and relative ion densities as the basic quantities. For $f_p^2 \gg f_c^2$, both ways lead to the same result provided that relative ion densities are measured correctly. For $f_p^2 \lesssim f_c^2$, the difference between the results depends on the discrepancy in measurements. Fig. 7 (discussed in more detail below) shows (among other things) a fairly good agreement between LHR frequency values calculated by using two different ways of electron density evaluation.

To obtain "along the orbit" values of f_{LHR}, we had to interpolate the values of two data sets from different instruments onto the same time scale. We treated IAP data timing as a basis and used linear interpolation of two electron density values adjacent to each ion density measurement. Having the electron and ion density values at the same place, we calculated f_{LHR} along all orbits during Demeter operation (about 34 000 orbits) using the expression (2).

Ionospheric plasma parameters are highly sensitive to solar activity. Therefore we have eliminated the data which correspond to periods of high solar activity, namely, when K_p index was greater than 3. All f_{LHR} measurements have been arranged in a 180×120 matrix that corresponds to a global map $180^\circ \times 360^\circ$ with $1^\circ \times 3^\circ$ resolution, separately for day/night and for every month of Demeter operation. Then, a certain number of f_{LHR} falls within each bin. Thereby, we have 5-dimensional matrix: the 1st and the 2nd positions correspond to geomagnetic latitude and longitude of the bin $\{i,j\}$, respectively, the 3d index gives Local Time LT (10:30/22:30—day/night), the 4th corresponds to month number (7×12 months of DEMETER operation from January 2004 to December 2010) {month}, and the 5th index refers to a given f_{LHR} value that falls within this bin $\{N\}$. One month of averaging is chosen to provide more or less uniform coverage of the data (which still have blank spaces due to the very small bin size). Having monthly maps, we are able to accumulate the f_{LHR} values in the seasons over several years. For example, to present a global distribution of f_{LHR} over spring night, one must accumulate within every bin all f_{LHR} values from March, April and May for certain years of interest and calculate the quantity

$$\langle (f_{\mathrm{LHR}})_{ij}^{\mathrm{LT}} \rangle, \tag{4}$$

where $\langle \ldots \rangle$ stands for the median value over {month} and $\{N\}$. Due to the solar activity cycle, yearly variation of ionospheric plasma parameters does not replicate from year to year. In order to take into account these yearly variations, only "similar" years have been considered for such an accumulation. It means that during these years, ionospheric plasma parameters (for example, electron density) vary in quite a similar way. A three year period from 2007 to 2009 has been chosen to represent f_{LHR} global distribution in different seasons, in the daytime and in the nighttime. Global maps of f_{LHR} above seismic regions were created in a similar way. Only data that fall in the area near the gathering earthquakes (square area around an earthquake $6^\circ \times 6^\circ$), 5 days before up to the earthquake occurrence were included. The corresponding values of f_{LHR} are called here

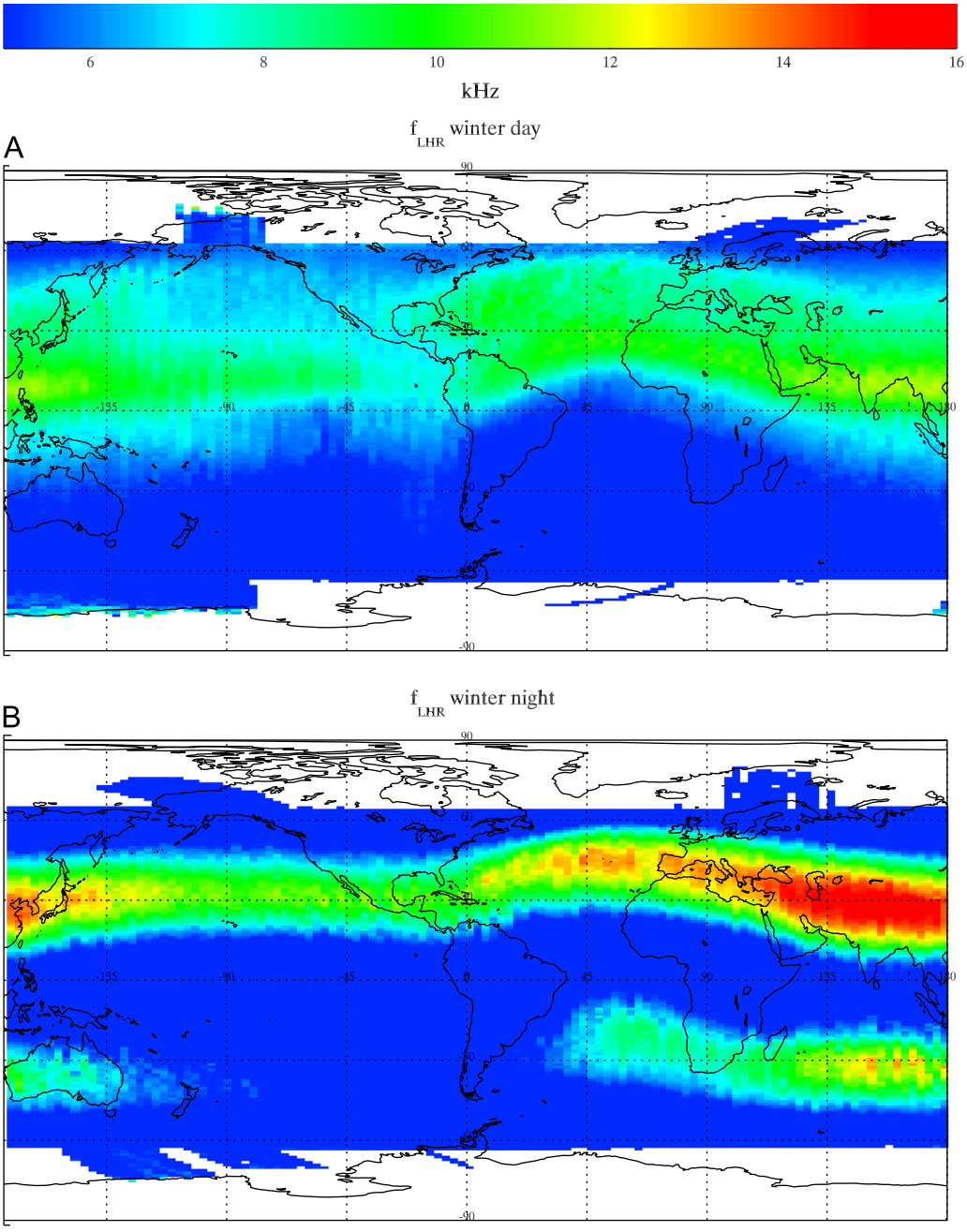

Fig. 1. Map of LHR frequency for winter.

"with EQ" (f_{LHREQ}). The maps of f_{LHR} that were constructed from all data except those related to earthquakes are called as "background". The earthquake database was taken from the US geological survey server http://earthquake.usgs.gov/earthquakes/eqarchives/epic/. Only the earthquakes with magnitudes 5 and greater were considered. The maps of LHR frequency and its variations related to earthquakes are discussed in the next section.

5. Maps of LHR frequency and VLF transmitter signal intensity: DEMETER observations

The main idea behind our suggestion on earthquake warning consists in the following. The amplitude of transmitter signal observed in the opposite hemisphere depends crucially on whether the frequency is higher or lower than the maximal LHR frequency above observation regions. This notion follows from theoretical consideration of LHR reflection of non-ducted signals, while its experimental proof is presented below. Figs. 1 and 2 show the maps of LHR frequency over the globe calculated from DEMETER data for winter (day and night) and summer (day and night), respectively. These and the following maps are plotted in geomagnetic coordinates. We should underline that the seasons indicated in the figures refer to the Northern hemisphere, but, when discussing seasonal variations of LHR frequency, we refer to the seasons in the hemisphere under discussion. According to the measurement, the LHR frequency varies in a wide range from few kHz up to 16–18 kHz. In general, LHR frequency is larger in winter than in summer, and also, it is larger during the night-time than during the daytime.

Further on, we will discuss the observations of VLF signals from Alpha transmitters, which are situated close to Krasnodar,

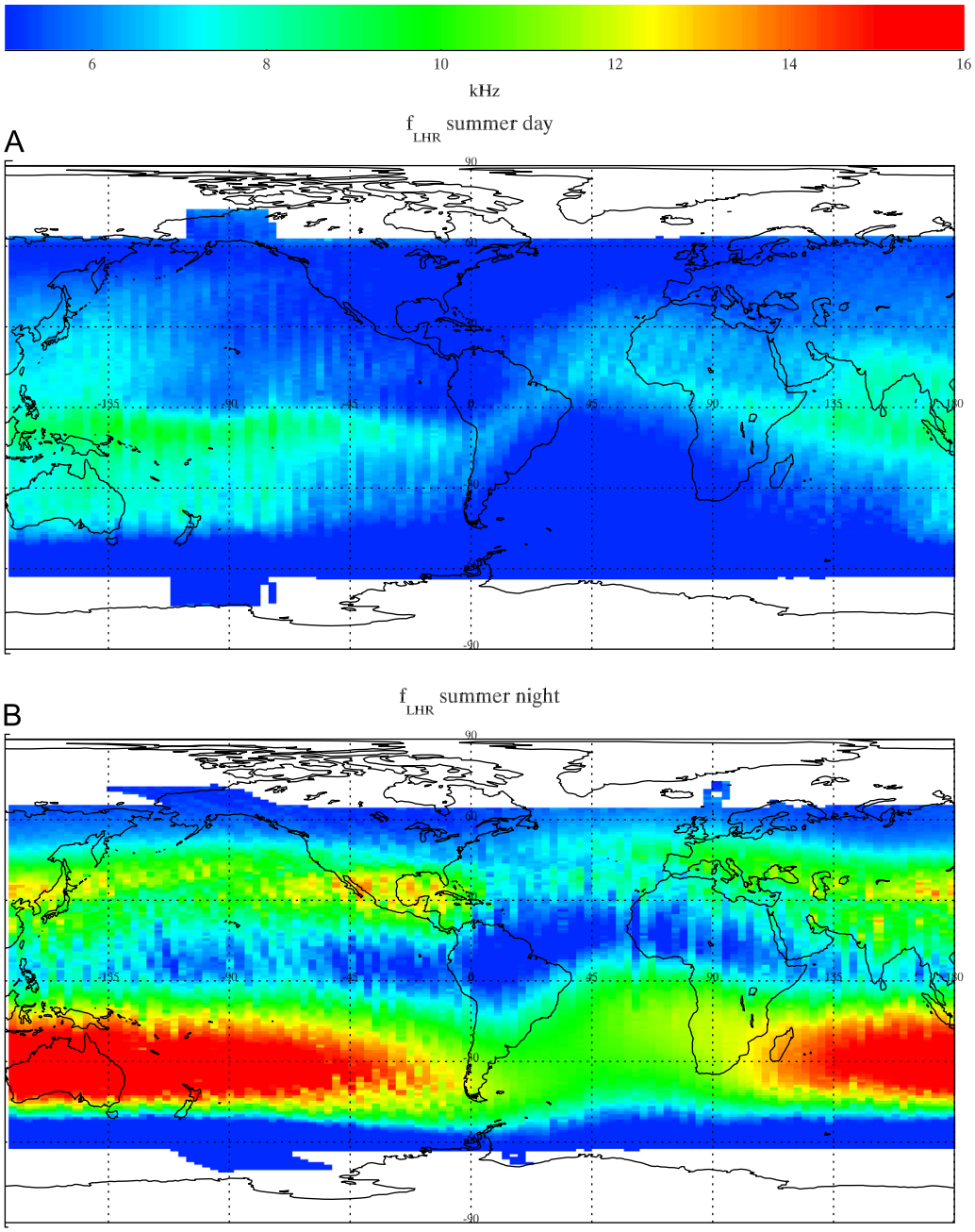

Fig. 2. Map of LHR frequency for summer.

Novosibirsk, and Komsomol'sk-na-Amure, each operating at three frequencies: 11.9, 12.6, and 14.9 kHz. Figs. 3 and 4 show maps of spectral intensity in narrow bands around transmitter signal frequencies 11.9 and 14.9 kHz, for winter day and winter night, respectively. The maps were obtained in the same way as the maps of LHR frequency with the exception that $1^\circ \times 1^\circ$ grid over latitude and longitude was used in this case. For the sake of definiteness, let us consider Novosibirsk transmitter. Its magnetically conjugated region is situated in the S hemisphere and has geomagnetic coordinates (47°S, 160°E). The LHR frequency is ~(5–6) kHz (northern winter, day), ~(10–11) kHz (northern winter, night), ~(6–7) kHz (northern summer, day), and ~(12–13) kHz (northern summer, night), as it is seen from Figs. 1 and 2. We notice that, in both winter and summer, the day values of f_{LHR} are below all frequencies of Alpha transmitters, while during the night time, 11.9 kHz$\lesssim(f_{LHR})_{max} <$ 14.9 kHz. Thus, during the day time, neither 11.9 kHz nor 14.9 kHz wave suffers LHR reflection, and their amplitudes in the conjugated region should be close, which is confirmed by Fig. 3. On the contrary, during the night-time, 11.9 kHz waves do, while 14.9 kHz waves do not suffer LHR reflection, thus, the amplitudes of 14.9 kHz waves should be larger than the amplitudes of 11.9 kHz waves. Fig. 4 provides the experimental proof of this relation. For summer time, electric field intensity at two chosen frequencies shows similar behaviour.

Before proceeding to further discussion of the experimental data, an important remark is in order. We treat VLF transmitter signals as a diagnostic tool which presumably does not modify the medium properties, at least those of them which we use, namely, the LHR frequency profile in the hemisphere opposite to that of the transmitter site. At the same time, VLF transmitter signals can potentially modify the ionospheric plasma and cause man-made effects that should be distinguished from natural ionospheric disturbances. The most obvious way by which a transmitter signal can modify the ionosphere is wave induced precipitation of

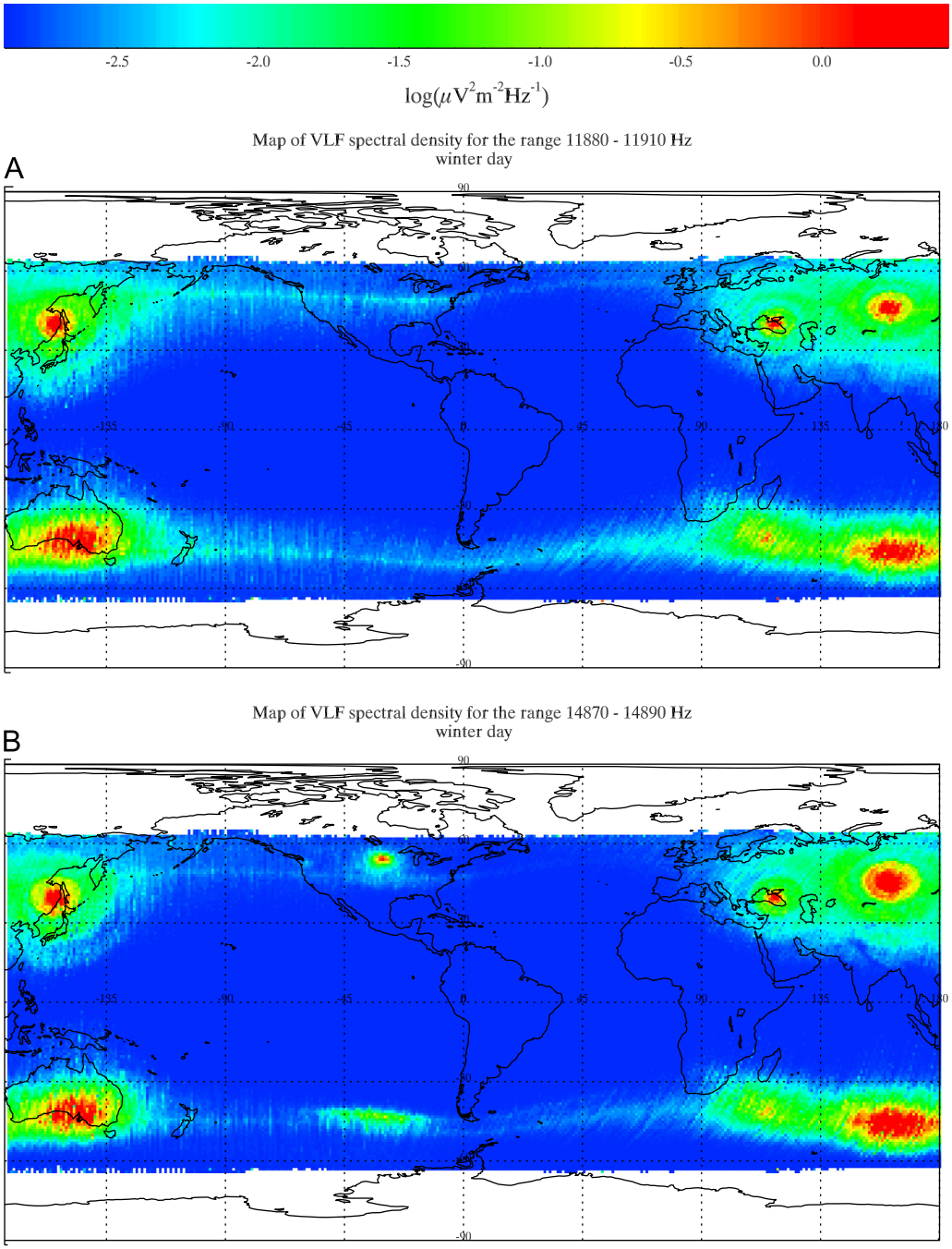

Fig. 3. Maps of electric field spectral intensity at about 11.9 and 14.9 kHz for winter day.

energetic particles caused by their resonant interaction with the whistler-mode wave (transmitter signal) in the magnetosphere (see e.g. Shklyar, 1986, the review by Shklyar and Matsumoto, 2009, and references therein). For energetic electrons near the loss-cone boundary, this interaction can scatter (or diffuse) them into the loss cone with subsequent precipitation into the atmosphere creating new free electrons (e.g. Karpman and Shklyar, 1977; Imhof et al., 1983; Pradipta et al., 2007). However, as it has been shown by Bell et al. (2011) on the basis of DEMETER data, even the most powerful VLF transmitters such as Australian NWC and American NAA do not produce significant large-scale variations of plasma density and temperature in the conjugate region.

A more subtle mechanism of ionospheric plasma modification by VLF transmitter signal has been put forward by Labno et al. (2007). It includes the parametric process in which a whistler-mode wave (transmitter signal) excites two quasi-resonance whistler-mode waves (often called lower hybrid resonance (LHR) waves, although their frequency may be much larger than the LHR frequency, as it is the case under conditions considered by Labno et al., 2007), and a zero frequency plasma mode. The excited LHR waves can, according to Labno et al. (2007), interact and accelerate suprathermal electrons in the region over the transmitter. The parametric process described above operates when the corresponding matching relations together with dispersion relations for all modes involved are satisfied. In an inhomogeneous plasma these conditions cannot be fulfilled throughout an extended interaction region, which makes the process under discussion important only for a very large amplitude of pumping wave, which

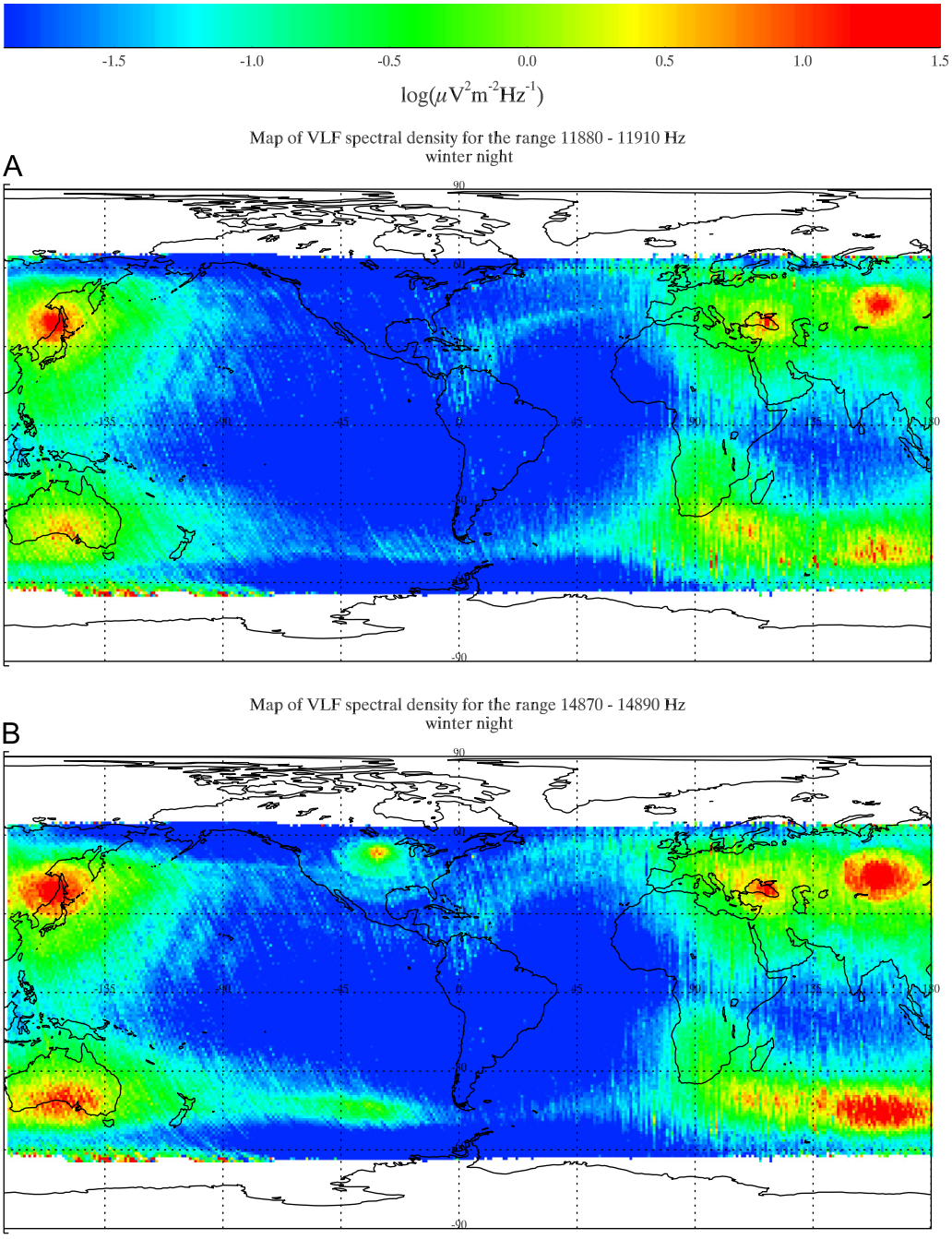

Fig. 4. Maps of electric field spectral intensity at about 11.9 and 14.9 kHz for winter night.

is hardly achieved for Alpha transmitters that we use in our study. We should mention that excitation of LHR waves due to VLF transmitter signal scattering on small scale plasma density irregularities in the ionosphere has been considered, e.g. by Bell and Ngo (1990) and Shklyar and Washimi (1994). In all cases, the processes mentioned above take place permanently, together with the operation of Alpha transmitters, independently of other possible processes related to gathering earthquakes. Thus, the corresponding variations are included in the "background" state.

6. LHR frequency above seismic regions

A matter of principle is the behaviour of the LHR frequency before an earthquake. Here we present for the first time an experimental study on this matter. Using the DEMETER data, we have calculated relative variations X of the LHR frequency in relation to earthquakes

$$X = \frac{\langle f_{\mathrm{LHREQ}}\rangle - \langle f_{\mathrm{LHR}}\rangle}{\langle f_{\mathrm{LHR}}\rangle}, \tag{5}$$

where f_{LHREQ} is the quantity defined above (see the end of Section 4), f_{LHR} is the LHR frequency excluding the periods before earthquakes, and $\langle\ldots\rangle$ stands for median values of the corresponding quantities for 3 yr from 2007 to 2009. The quantity X which is associated with the place of earthquake occurrence is visualised on the maps by colours according to the colour bar. The corresponding map is shown on the lower panel in Fig. 5, while the upper panel displays the background LHR frequency above the same regions, which we denote by "f_{LHR} above seismic region." To facilitate the observation of seismically

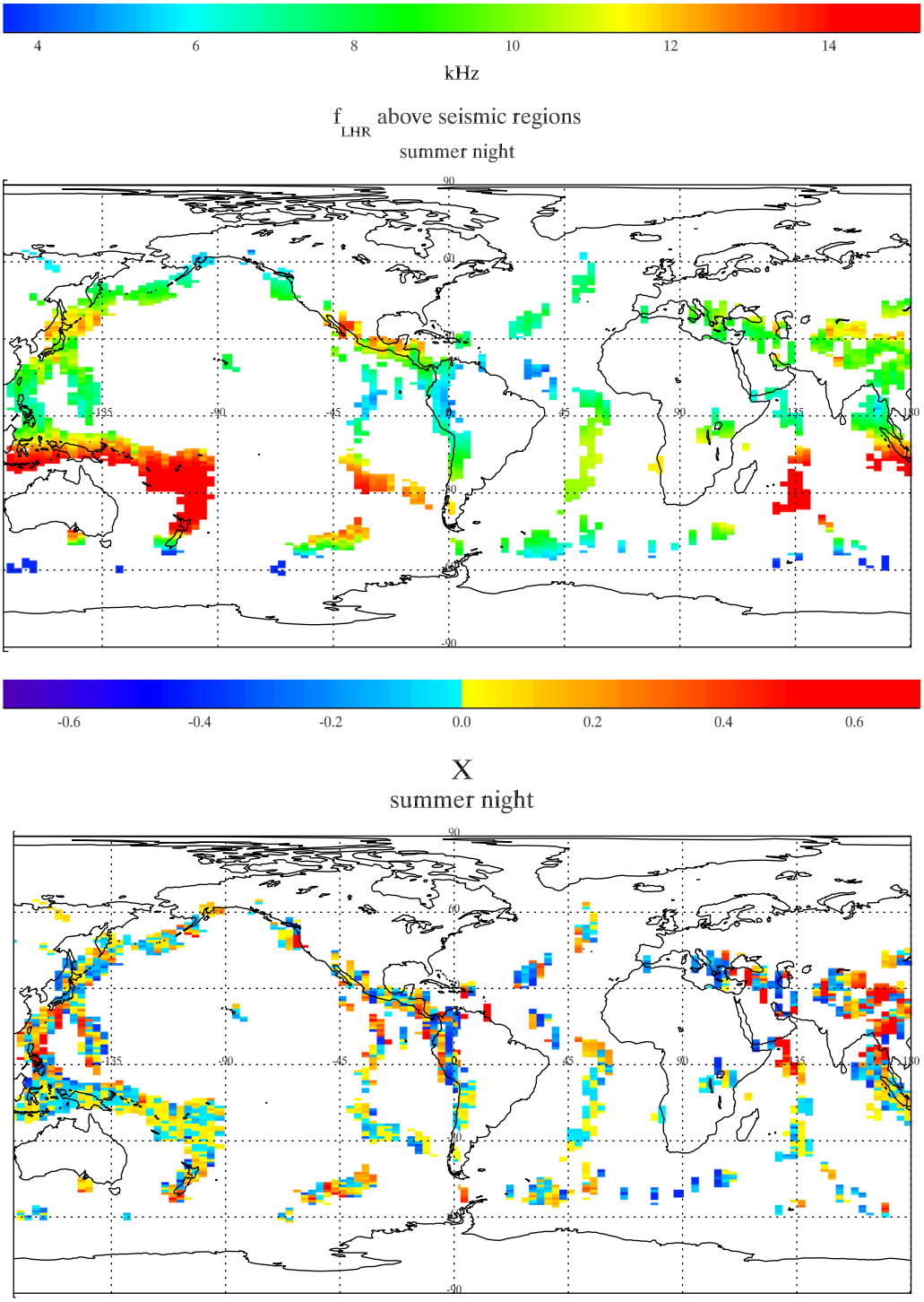

Fig. 5. Maps of the quantities f_{LHR} above seismic regions (upper panel) and X (bottom panel) for summer night periods. (For interpretation of the references to color in this figure caption, the reader is referred to the web version of this article.)

active regions over the globe, we use geomagnetic coordinates with marked contour of continents. The analysis of data has shown that during night-time the quantity X may have a significant value up to 0.6, while in the daytime the quantity X is close to zero. That is why hereinafter we discuss only night-time maps. We see that both blue colours (corresponding to a decrease of the LHR frequency before earthquakes) and red colours (corresponding to an increase of the LHR frequency before earthquakes) are present on the bottom panel in Fig. 5, thus, a definite variation of this quantity is not revealed. Despite the absence of a regular variation of the LHR frequency before earthquakes, its essential change in the night-time indicates the influence of gathering earthquakes on plasma distribution in the night-time ionosphere.

For quantitative characterisation of the relation between the LHR frequency over seismic region and its variations before gathering earthquakes, we have carried out a statistical analysis of the measurements of f_{LHR} above few regions known to be seismically active. Specifically, we have considered five $20^\circ \times 20^\circ$ square areas around Chile (20°S, 0°E), Japan (30°N, 150°W), Philippines (10°S, 160°W), Solomon Islands (20°S, 125°W), and

Sumatra (10°S, 170°E), examining only those measurements of f_{LHR} that fell into these areas.

The results for Chile region corresponding to summer night periods are shown in Fig. 6. The upper panel shows the background distribution of f_{LHR} values (blue line) and the distribution of f_{LHREQ} values before earthquakes as described above (red line). As one can see, the distributions of both quantities cover very wide frequency bands and are significantly different from normal distribution, which is not surprising because the measurements cover wide intervals in both latitude and time. The median value in the background distribution is shown by dashed blue line. The median frequency in this case is equal to ~9.3 kHz. Two solid blue lines comprise 80% of cases in the background distribution, with 10% of cases outside of each line. For quantitative characteristic of differences between two distributions, we have examined the

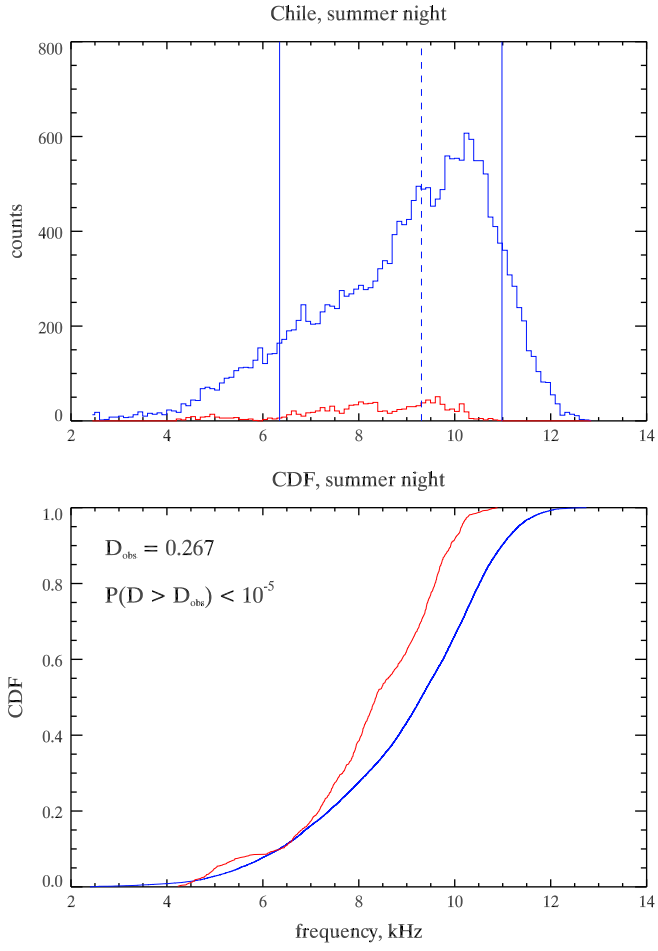

Fig. 6. Statistical analysis of f_{LHR} distributions relation to earthquakes above Chile region. (For interpretation of the references to color in this figure caption, the reader is referred to the web version of this article.)

value β_p which is the relative number of cases from f_{LHREQ} distribution below the p-quantile ($0 < p < 1$) of the f_{LHR} distribution. In these terms, the median for the f_{LHR} distribution is 0.5-quantile, and two solid lines described above are 0.1- and 0.9-quantiles. The values of β_p for the given example shown in Fig. 6 are $\beta_{0.1} = 0.1$, $\beta_{0.5} = 0.7$, $\beta_{0.9} = 1.0$, which suggests that the probability of observation of low f_{LHR} values before earthquakes remains the same as in the background distribution, while the probability of observation of high f_{LHR} values decreases.

The lower panel shows the empirical cumulative distributional functions (CDF), $F_n(f)$ and $G_m(f)$, derived from two distributions shown on the upper panel, namely, of f_{LHR} (blue) and f_{LHREQ} (red), respectively. The numbers of measurements in these distributions are denoted by n and m. CDF is, in fact, the relative number of cases (y-axis) in which f_{LHR} is below the given value (x-axis). Analysis of CDF allows us to track the portion of measurements of f_{LHR} below the given level, and to evaluate deviation of "disturbed" distribution from the background one.

To test whether these distributions differ, we apply the Kolmogorov–Smirnov test. In two-sample case, the Kolmogorov–Smirnov statistic is

$$D_{obs} = \sup_f |F_n(f) - G_m(f)|. \quad (6)$$

The significance level of an observed value of D (as a disproof of the null hypothesis that the distributions are the same) is given approximately by the formula (see e.g. Stephens, 1970)

$$P(D > D_{obs}) = Q_{KS}([\sqrt{N_{eff}} + 0.12 + 0.11/\sqrt{N_{eff}}]D_{obs}), \quad (7)$$

where

$$Q_{KS}(\lambda) = 2\sum_{j=1}^{\infty}(-1)^{j-1}e^{-2j^2\lambda^2},$$

and

$$N_{eff} = \frac{nm}{n+m}.$$

For the given case shown in Fig. 6, null hypothesis is rejected at the level less than 10^{-5}, while the Kolmogorov–Smirnov statistic $D_{obs} = 0.267$, meaning that two distributions differ significantly.

The results of statistical analysis for all five considered regions are summarised in Table 1. The numbers given for each region and each season indicate, quite approximately, the quantity $\delta(f_{LHR}) \equiv G_m(f_{LHR}) - F_n(f_{LHR})$, which characterises the deviation of the CDF before earthquakes from the background CDF, and the interval of frequencies where this deviation is observed. A dash means that $|\delta(f_{LHR})| < 0.1$, which is observed in more than ~50% of cases. As one can see, in most cases where the difference between the distribution functions is significant, the quantity $\delta(f_{LHR})$ is positive, reaching the values up to 0.35. We should stress that the difference between two CDFs pointed out above reveals only in specific frequency intervals that, in turn, depend on the region and

Table 1
Results of statistical analysis of the CDF before earthquakes deviation from the background CDF.

Seasons\Regions	Chile	Japan	Philippines	Solomon Isl.	Sumatra
Winter	0.25 $f \approx 3$ kHz	–	–	0.1–0.2 4 kHz $< f_{LHR} <$ 5 kHz	–
Spring	0.15–0.2 5 kHz $< f_{LHR} <$ 8 kHz	–	–	–	–
Summer	0.15–0.25 8 kHz $< f_{LHR} <$ 11 kHz	–	–	0.15–0.2 15 kHz $< f_{LHR} <$ 17 kHz	–
Autumn	0.15–0.35 3 kHz $< f_{LHR} <$ 7 kHz	−0.1−−0.2 10 kHz $< f_{LHR} <$ 15 kHz	–	~0.1 5 kHz $< f_{LHR} <$ 10 kHz	–

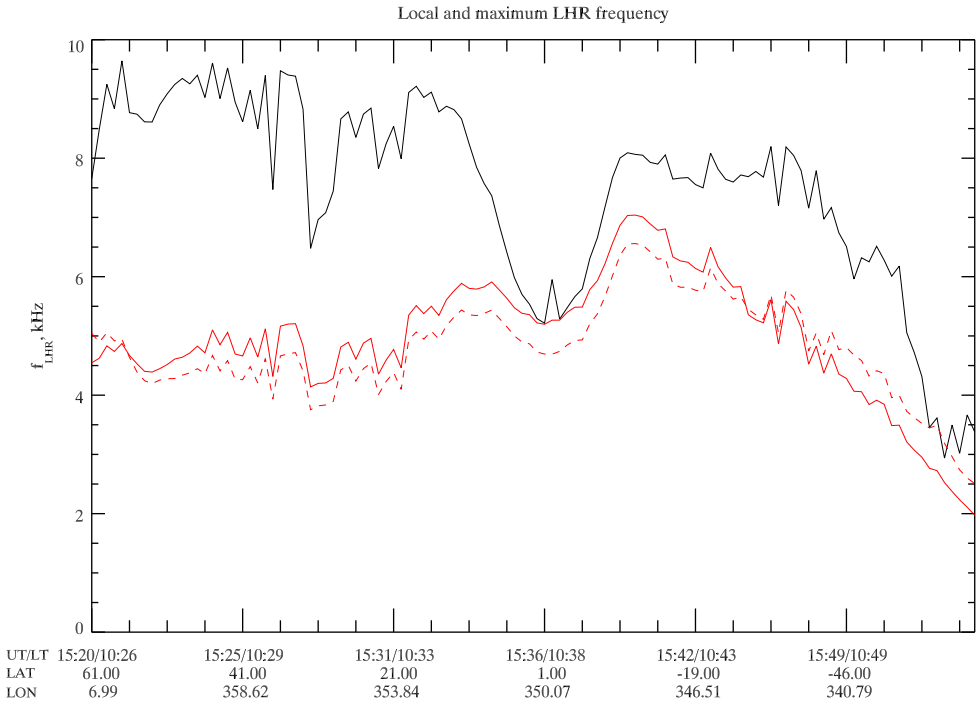

Fig. 7. Local (red lines) and maximum (black line) LHR frequency along the DEMETER orbit 15000_0. The data were taken on 24 April 2007. (For interpretation of the references to color in this figure caption, the reader is referred to the web version of this article.)

season. Another interesting observation consists in that $|\delta(f_{LHR})|$ is negligible for equatorial latitudes (Philippines, Sumatra) and is significant for higher latitudes (Chile, Solomon Islands).

7. Discussion and conclusions

We have presented the maps of the lower hybrid resonance (LHR) frequency, f_{LHR}, over the globe for various seasons and time of the day based on DEMETER data for 3 yr. Special consideration has been given for the corresponding quantity over seismic regions and its variations before gathering earthquakes using the earthquake database from the US geological survey server. We found that the distributions of f_{LHR} with and without earthquakes are meaningly different above several seismic regions. This suggests a new method of monitoring unusual variations of plasma parameters in the lower ionosphere, possibly related to gathering earthquakes. The method relies upon peculiarities of quasi-resonance whistler-mode wave propagation in the magnetosphere and upper ionosphere, in the LHR frequency band. VLF transmitter signals propagating over magnetospheric trajectories in non-ducted regime are known to fall into this category of whistler-mode waves. Such a wave cannot propagate in the region where its frequency f is below the LHR frequency f_{LHR}, thus, if the wave propagates from the magnetosphere to the ionosphere, i.e. in the direction of increasing f_{LHR}, it will be reflected from the region where $f \lesssim f_{LHR}$ provided that $f < (f_{LHR})_{max}$, where $(f_{LHR})_{max}$ is the maximum LHR frequency in the upper ionosphere along the wave path. This wave will not be registered on the ground or/and on a low-altitude satellite like DEMETER orbiting below the LHR maximum; at least the amplitude of the signal will be very low. On the contrary, if $f > (f_{LHR})_{max}$, the signal will be registered on low-altitude satellites, and its amplitude on the ground should be higher than in the case $f < (f_{LHR})_{max}$, provided that the conditions of wave exit to the ground exist at all. This conception has been verified on the basis of the LHR maps and spectral maps (related to Alpha transmitters) calculated from the DEMETER data.

Since the LHR frequency, even for given region, season, and time of the day varies in a wide range, and since the character of its variation is not unique, the method of monitoring its variations should include multiple measurements during an extended period of time. The performed study gives us the probability (related to unperturbed conditions) of observation of fixed frequency signal from a VLF transmitter situated in the region magnetically conjugated to the observation point, i.e. the probability that the maximum of the LHR frequency above the observation point is less than the transmitter frequency. If for the same region, season, and time of the day the relative number of cases when the transmitter signal is observed differs essentially from the "unperturbed" probability, it means that during the observation period the LHR frequency suffers unusual variations. Needless to say that a gathering earthquake is only one possible cause of such variations.

We should mention that DEMETER measurements which constitute the basis of the present study give us a local but not the maximum values of the LHR frequency. In our arguments we assume that the maximum LHR frequency varies synchronously with the local one, and their seasonal, diurnal, and pre-earthquake variations are similar. The reasonableness of these assumptions is illustrated by Fig. 7, which shows the graphs of local (red) and maximum (black) LHR frequency along one orbit, calculated with the help of diffusive equilibrium model. The calculations use the concentrations of various ion species at the base level (DEMETER altitude) and ion temperature measured by IAP, and the measured electron temperature, of course. The values of local LHR frequency calculated by using two ways of electron density evaluation are shown by solid ($n_e = \sum n_i$) and dashed (n_e obtained from ISL measurements) red lines, which are quite close.

The second key point in our consideration refers to significant modification of LHR frequency profile, including the value of LHR maximum, in response to relatively small variations of ionospheric parameters, in particular, absolute and relative contents of ion species on a "base level" in the ionosphere. In this way, the amplitude of VLF transmitter signal, which is very sensitive to

the relation between f and $(f_{LHR})_{max}$, becomes very sensitive to variations of ionospheric parameters.

Since there were no convincing evidences in the literature concerning the variations of the LHR frequency before earthquakes, we have undertaken a research into this subject based on DEMETER data. The results have shown that the LHR frequency before earthquakes can both decrease and increase. The performed statistical analysis has shown that the distributions of the LHR frequency with and without earthquakes over certain seismic regions are significantly different.

In sum, the results of this study suggest a method of revealing unusual variations of ionospheric parameters possibly related to a gathering earthquake, by monitoring the amplitudes of VLF transmitter signals with specially chosen frequencies and locations. Since these variations may be caused by reasons other than a gathering earthquake, they should only be considered as an additional indicator to be weighed along with other earthquake precursors.

Acknowledgments

This study has been performed under the 7th Framework Programme of the European Union, FP7-SPACE-2010-1, Grant agreement number 262005. The work is based on observations with the electric field experiment, the Langmuir probe ISL, and the plasma analyser IAP embarked on the micro-satellite DEMETER launched by CNES. The authors thank J.J. Berthelier and J.P. Lebreton for the use of these data, and David Píša for providing continent contour map in geomagnetic coordinates. The authors would also like to acknowledge the unknown reviewers for their comments and suggestions on improving the paper.

References

Afonin, V.V., Molchanov, O.A., Kodama, T., Hayakawa, M., Akentieva, O.A., 1999. Statistical study of ionosphere plasma response to seismic activity: search for reliable result from satellite observations. In: Hayakawa, M. (Ed.), Atmospheric and Ionospheric Electromagnetic Phenomena Associated with Earthquakes. Terra Scientific Publishing Company, Tokyo, pp. 597–618.

Alekhin, Ju.K., Shklyar, D.R., 1980. Some questions of electromagnetic wave propagation in magnetosphere. Geomagnetism i Aeronomia 20 (3), 501–507.

Angerami, J.J., Thomas, J.O., 1964. Studies of planetary atmospheres, 1. The distribution of electrons and ions in the Earth's exosphere. Journal of Geophysical Research 69, 4537–4560.

Bell, T.F., Ngo, H.D., 1990. Electrostatic lower hybrid waves excited by electromagnetic whistler mode waves scattering from planar magnetic-field-aligned plasma density irregularities. Journal of Geophysical Research 95, 149–172.

Bell, T.F., Graf, K., Inan, U.S., Piddyachiy, D., Parrot, M., 2011. DEMETER observations of ionospheric heating by powerful VLF transmitters. Geophysical Research Letters 38, L11103, http://dx.doi.org/10.1029/2011GL047503.

Berthelier, J.J., et al., 2006a. ICE, the electric field experiment on DEMETER. Planetary and Space Science 54, 456–471.

Berthelier, J.J., Godefroy, M., Leblanc, F., Seran, E., Peschard, D., Gilbert, P., Artru, J., 2006b. IAP the thermal plasma analyzer on DEMETER. Planetary and Space Science 54, 487–501.

Bošková, J., Šmilauer, J., Jiříček, F., Tříska, P., 1993. Is the ion composition of outer ionosphere related to seismic activity. Journal of Atmospheric and Terrestrial Physics 55 (13), 1689–1695.

Cerisier, J.C., 1973. A theoretical and experimental study of non-ducted VLF waves after propagation through the magnetosphere. Journal of Atmospheric and Terrestrial Physics 35 (1), 77–82.

Chmyrev, V.M., Isaev, N.V., Serebryakova, O.N., Sorokin, V.M., Sobolev, Ya.P., 1997. Small-scale plasma inhomogeneities and correlated ELF emissions in the ionosphere over an earthquake region. Journal of Atmospheric and Solar-Terrestrial Physics 59, 967–973.

Chmyrev, V.M., Sorokin, V.M., Shklyar, D.R., 2008. VLF transmitter signals as a possible tool for detection of seismic effects on the ionosphere. Journal of Atmospheric and Solar-Terrestrial Physics 70, 2053–2060.

Collier, A.B., Lichtenberger, J., Clilverd, M.A., Rodger, C.J., Steinbach, P., 2011. Source region for whistlers detected at Rothera, Antarctica. Journal of Geophysical Research 116, A03219, http://dx.doi.org/10.1029/2010JA016197.

Francis, S.H., 1975. Global propagation of atmospheric gravity waves: a review. Journal of Atmospheric and Solar-Terrestrial Physics 37, 1011–1054.

Gokhberg, M.B., Pilipenko, V.A., Pokhotelov, O.A., 1983. On seismic precursors in the ionosphere. Izvestiya USSR Academy of Sciences. Physics of the Earth Series 10, 17–21.

Grigor'ev, G.I., 1999. Acoustic-gravity waves in the Earth's atmosphere (review). Radiophysics and Quantum Electronics 42 (1), 1–21, http://dx.doi.org/10.1007/BF02677636.

Hayakawa, M., Molchanov, O.A. (Eds.), 2002. Seismo Electromagnetics: Lithosphere–Atmosphere–Ionosphere Coupling. TERRAPUB, Tokyo.

Hayakawa, M., Molchanov, O.A., Kodama, T., Afonin, V.V., Akentieva, O.A., 2000. Plasma density variations observed on a satellite possibly related to seismicity. Advances in Space Research 26 (8), 1277–1280.

Helliwell, R.A., 1965. Whistlers and Related Ionospheric Phenomena. Stanford University Press, Stanford, California.

Imhof, W.L., Reagan, J.Â., Voss, H.D., Gaines, E.E., Datlowe, D.W., Mobilia, J., 1983. Direct observation of radiation belt electrons precipitated by the controlled injection of VLF signals from a ground-based transmitter. Geophysical Research Letters 10, 361–364.

Karpman, V.I., Shklyar, D.R., 1977. Particle precipitation caused by a single whistler-mode wave injected into the magnetosphere. Planetary and Space Science 25, 395–403.

Kimura, I., 1966. Effects of ions on whistler-mode ray tracing. Radio Sciences 1 (3), 269–283.

Labno, A., Pradipta, R., Lee, M.C., Sulzer, M.P., Burton, L.M., Cohen, J.A., Kuo, S.P., Rokusek, D.L., 2007. Whistler-mode wave interactions with ionospheric plasmas over Arecibo. Journal of Geophysical Research 112, A03306, http://dx.doi.org/10.1029/2006JA012089.

Larkina, V.I., Migulin, V.V., Mogilevsky, M.M., Molchanov, O.A., Galperin, Yu.I., Jorjio, N.V., Gokhberg, M.B., Lefeuvre, F., 1984. Earthquake effects in the ionosphere according to Intercosmos-19 and Aureol-3 satellite data. In: Results of the ARCAD-3 Project and of the Recent Programmes in Magnetospheric and Inospheric Physics, Cepadues-Editions, Toulouse, pp. 685–699.

Larkina, V.I., Migulin, V.V., Molchanov, O.A., Kharkov, I.P., Inchin, A.S., Schvetcova, V.B., 1989. Some statistical results on very low frequency radiowave emissions in the upper ionosphere over earthquake zones. Physics of the Earth and Planetary Interiors 57 (1–2), 100–109.

Lebreton, J.-P., Strevak, S., Travnicek, P., Maksimovic, M., Klinge, D., Merikallio, S., Lagoutte, D., Poirier, B., Blelly, P.-L., Kozacek, Z., Salaquarda, M., 2006. The ISL Langmuir probe experiment processing onboard DEMETER: scientific objectives, description and first results. Planetary and Space Science 54, 472–486.

Lee, M.C., Pradipta, R., Burke, W.J., Labno, A., Burton, L.M., Cohen, J.A., Dorfman, S.E., Coster, A.J., Sulzer, M.P., Kuo, S.P., 2008. Did tsunami-launched gravity waves trigger ionospheric turbulence over arecibo? Journal of Geophysical Research 113, A01302, http://dx.doi.org/10.1029/2007JA012615.

Molchanov, O., Rozhnoi, A., Solovieva, M., Akentieva, O., Berthelier, J.J., Parrot, M., Lefeuvre, F., Biagi, P.F., Castellana, L., Hayakawa, M., 2006. Global diagnostics of the ionospheric perturbations related to the seismic activity using the VLF radio signals collected on the DEMETER satellite. Natural Hazards and Earth System Sciences 6, 745–753.

Parrot, M., Lefeuvre, F., 1985. Correlation between GEOS VLF emissions and earthquakes. Annales Geophysicae 3, 737–748.

Parrot, M., et al., 2006. The magnetic field experiment IMSC and its data processing onboard DEMETER: scientific objectives, description and first results. Planetary and Space Science 54, 441–455.

Pradipta, R., Labno, A., Lee, M.C., Burke, W.J., Sulzer, M.P., Cohen, J.A., Burton, L.M., Kuo, S.P., Rokusek, D.L., 2007. Electron precipitation from the inner radiation belt above Arecibo. Geophysical Research Letters 34, L08101, http://dx.doi.org/10.1029/2007GL029807.

Pulinets, S.A., Legenka, A.D., Gaivoronskaya, T.V., Dupuev, V.Kh., 2003. Main phenomenological features of ionospheric precursors of strong earthquakes. Journal of Atmospheric and Solar-Terrestrial Physics 65 (16–18), 1337–1347.

Pulinets, S.A., Liu, J.Y., Safronova, I.A., 2004. Interpretation of a statistical analysis of variations in the foF2 critical frequency before earthquakes based on data from Chung-Li ionospheric station (Taiwan). Journal of Geomagnetism and Aeronomy 44, 102–106.

Rozhnoi, A., Molchanov, O., Solovieva, M., Gladyshev, V., Akentieva, O., Berthelier, J.J., Parrot, M., Lefeuvre, F., Hayakawa, M., Castellana, L., Biagi, P.F., 2007. Possible seismo-ionosphere perturbations revealed by VLF signals collected on ground and on a satellite. Natural Hazards and Earth System Sciences 7, 617–624.

Santolík, O., Němec, F., Parrot, M., Lagoutte, D., Madrias, L., Berthelier, J.J., 2006. Analysis methods for multi-component wave measurements on board the DEMETER spacecraft. Planetary and Space Science 54, 512–527.

Serebryakova, O.N., Bilichenko, S.V., Chmyrev, V.M., Parrot, M., Rauch, J.L., Lefeuvre, F., Pokhotelov, O.A., 1992. Electromagnetic ELF radiation from earthquake region as observed by low-altitude satellites. Geophysical Research Letters 19, 91–94.

Shklyar, D.R., 1986. Particle interaction with an electrostatic VLF wave in the magnetosphere with an application to proton precipitation. Planetary and Space Science 34, 1091–1099.

Shklyar, D.R., Washimi, H., 1994. LHR wave excitation by whistlers in the magnetospheric plasma. Journal of Geophysical Research 99 (A12), 23,695–23,704.

Shklyar, D.R., Truhlik, V., 1998. On the modification of light ion concentration profiles above seismically active regions: a qualitative consideration. Journal of Atmospheric and Solar Terrestrial Physics 60 (10), 1025–1033.

Shklyar, D.R., Chum, J., Jiříček, F., 2004. Characteristic properties of Nu whistlers as inferred from observations and numerical modelling. Annales Geophysicae 22, 3589–3606.

Shklyar, D.R., Matsumoto, H., 2009. Oblique whistler-mode waves in the inhomogeneous magnetospheric plasma: resonant interactions with energetic charged particles. Surveys in Geophysics 30, 55–104.

Shklyar, D.R., Parrot, M., Chum, J., Santolik, O., Titova, E.E., 2010. On the origin of lower- and upper-frequency cutoffs on wedge-like spectrograms observed by DEMETER in the midlatitude ionosphere. Journal of Geophysical Research 115, A05203, http://dx.doi.org/10.1029/2009JA014672.

Solovieva, M.S., Rozhnoi, A.A., Molchanov, O.A., 2009. Variation in the parameters of VLF signals on the DEMETER satellite during the periods of seismic activity. Geomagnetism and Aeronomy 49 (4), 532–541.

Stephens, M.A., 1970. Use of the Kolmogorov–Smirnov, Cramer–Von Mises and related statistics without extensive tables. Journal of the Royal Statistical Society, Series B (Methodological) 32 (1), 115–122.

Storey, L.R.O., 1953. An investigation of whistling atmospherics. Philosophical Transactions of the Royal Society of London A246 (908), 113–141.

Walker, A.D.M., 1976. The theory of whistler propagation. Reviews of Geophysics 14 (4), 629–638.

Walter, F., Angerami, J.J., 1969. Nonducted mode of VLF propagation between conjugate hemispheres; Observations on OGO's 2 and 4 of the 'Walking-Trace' whistler and of doppler shifts in fixed frequency transmissions. Journal of Geophysical Research 74 (26), 6352–6370.